Distortion-free broadband holograms: A novel class of elements utilizing the wavelength-independent geometric phase

Xiao Xiang, Matthew N. Miskiewicz and Michael J. Escuti

Dept. Electrical and Computer Engineering, North Carolina State University, Raleigh, USA

ABSTRACT

We demonstrate a novel class of elements called Far-Field Geometric Phase Holograms (FGPH) capable of producing far-field output images free of chromatic distortion for a broad range of input wavelengths. The FGPH utilizes the geometric phase which applies the same phase profile to any incident wave regardless of wavelength. Thus, the fidelity of an image produced by an FGPH is the same for all wavelengths. However, being a diffractive element, the FGPH is still dispersive in that the size of a generated image depends on the replay wavelength according to the diffraction equation. In this paper, we give theory for the ideal FGPH element, describing its replay characteristics and unique polarization properties. We experimentally realize an FGPH element using photo-aligned liquid crystals patterned with a direct-write system. We characterize the fabricated element and show the theory to be valid. Generally, this new class of polarization sensitive elements can produce broadband undistorted images with high diffraction efficiency.

Keywords: geometric phase, Fourier transform hologram

1. INTRODUCTION

We report an experimental generation and analysis of 2D computer generated Fourier geometric phase hologram. The geometric phase[1–3] of the hologram is generated by computer and recorded by a direct-write photo-alignment system.[4] Wavelength and polarization dependence of the hologram are studied both in theory and experiment. Simulation and experimental results are given for the unique properties of FGPH. Undistorted scaled image is observed for light with different wavelengths and polarization sensitivity is also examined. The results are in good agreement with theoretical prediction and verify that our FGPH has expected properties.

2. BACKGROUND

2.1 Fourier Transform Hologram

In a traditional computer generated Fourier Transform hologram(FTH)[5–8] the reconstruction of the image occurs in the far field. Generally, there are two steps in this process: computing the light field in the observer plane based on the target image, and then retrieve the phase or amplitude profile on the hologram plane for a phase hologram using certain algorithm.[9,10] Usually, the phase here is referred to the dynamic phase which depends on the wavelength. So this kind of hologram[11] works for single wavelength and chromatic distortion will occur if the wavelength is different. Additionally, traditional Fourier transform hologram is not sensitive to polarization, which means we cannot control the reconstructed image by polarization.

2.2 Geometric Phase

Geometric phase is the phase difference acquired over the course of a cycle or closed path, where the amount of acquired phase depends on the path traveled. For the polarized light, its geometric phase is changed when the polarization state is changed which can be understood with a path on the Poincaré Sphere.[12] Since the geometric phase is gained by the change in polarization rather than the difference in optical path, it is wavelength independent and polarization sensitive. This critical difference from dynamic phase results in some unique properties of geometric phase elements.[13–15]

Practical Holography XXIX: Materials and Applications, edited by Hans I. Bjelkhagen,
V. Michael Bove Jr., Proc. of SPIE, Vol. 9386, 938609 · © 2015 SPIE
CCC code: 0277-786X/15/$18 · doi: 10.1117/12.2084722

3. THEORY

Geometric phase holograms[16,17] are a new category of holograms that work upon the geometric phase of optical fields. The geometric phase is gained when the polarization state of light changes along a path on the Poincaré Sphere. Basically, the geometric phase is wavelength independent and has opposite sign for left and right circularly polarized light. In our FGPH, we modulate the geometric phase by a liquid crystal polymer film of which the optical axis is patterned according to the target phase.

To understand how the FGPH works, we can firstly consider the output electric field after passing though a retarder with the optical axis θ. Here we assume the input light is right circular polarized (RCP) and d is the thickness of the retarder with birefringence Δn,

$$\mathbf{E}_{output}(x',y',0) = \mathrm{E_{input}(x',y')}\frac{e^{i\phi_0}}{2\sqrt{2}}[(e^{i2\pi\zeta}+1)\begin{pmatrix}1\\ i\end{pmatrix} + (e^{i2\pi\zeta}-1)e^{i2\theta}\begin{pmatrix}1\\ -i\end{pmatrix}], \tag{1}$$

where $\phi_0 = 2\pi n_0/\lambda$, $\zeta = \Delta n d/\lambda$. The first term has the same polarization state as the input light but no information of the optical axis. The FGPH we fabricate is basically a film with plenty of tiny retarders with patterned local optical axis $\theta(x',y')$. The geometric phase $\phi_g(x',y') = 2\theta(x',y')$, and it is modulated by the hologram. The electric field for RCP input after passing through the hologram is then given by:

$$\mathbf{E}_{hologram}(x',y',0) = \frac{e^{i\phi_0}}{2\sqrt{2}}[(e^{i2\pi\zeta}+1)\begin{pmatrix}1\\ i\end{pmatrix} + (e^{i2\pi\zeta}-1)e^{i2\theta(x',y')}\begin{pmatrix}1\\ -i\end{pmatrix}], \tag{2}$$

where we neglect the initial phase and amplitude of the input light.

Given the well-known diffraction equation for far field, we can get the electric field at the image plane:

$$\mathbf{E}_{image}(x,y,z) = \frac{e^{ikz}}{i\lambda z}e^{i\frac{\pi}{\lambda z}(x^2+y^2)}\mathcal{F}[e^{i\phi_g(x',y')}]\begin{pmatrix}1\\ -i\end{pmatrix}, \tag{3}$$

where the zero order and the coefficient of the diffraction order is omitted and the $\mathcal{F}$ stands for Fourier transform.

3.1 Wavelength Dependence

Based on the result given above, we can rewrite the electric field at the image plane with $\xi = \frac{x}{\lambda z}$ and $\eta = \frac{y}{\lambda z}$,

$$\mathbf{E}_{image}(x,y,z) = \mathbf{E}(\xi,\eta), \tag{4}$$

Since the geometric phase $\theta(x',y')$ is independent of wavelength, we can write the electric field of certain wavelength λ_1 and λ_2 at the image plane respectively,

$$\mathbf{E}_{\lambda_1}(\xi_1,\eta_1) = \mathbf{E}(\frac{x}{\lambda_1 z},\frac{y}{\lambda_1 z}) \tag{5}$$

$$\mathbf{E}_{\lambda_2}(\xi_2,\eta_2) = \mathbf{E}(\frac{x}{\lambda_2 z},\frac{y}{\lambda_2 z}), \tag{6}$$

If we define the ratio of these two wavelengths $\alpha \equiv \frac{\lambda_1}{\lambda_2}$ and neglect the difference in the amplitude, we can rewrite that

$$\mathbf{E}_{\lambda_2}(\xi_2,\eta_2) = \mathbf{E}_{\lambda_1}(\alpha\xi_1,\alpha\eta_1) \tag{7}$$

From here we can see clearly that the image of the λ_2 is basically a scaled image of that given by λ_1 without any chromatic distortion involved.

3.1.1 Polarization Dependence

Since the geometric phase is polarization sensitive and thus opposite circular polarization state has opposite sign of phase, the output image of FGPH will be different given different polarized input light. If we neglect the zero order which always has the same polarization as the input light, the corresponding electric fields of RCP and LCP input are:

$$\mathbf{E}_{RCP}(x,y,z) = \mathcal{F}[e^{i\phi_g(x',y')}] \begin{pmatrix} 1 \\ -i \end{pmatrix} \tag{8}$$

$$\mathbf{E}_{LCP}(x,y,z) = \mathcal{F}[e^{-i\phi_g(x',y')}] \begin{pmatrix} 1 \\ i \end{pmatrix}, \tag{9}$$

where we omit the coefficient of the electric field and emphasize the polarization dependence of FGPH. From the result above, we can know that for circular polarized light its polarization state will flip and the diffraction angle of RCP and LCP input light will be opposite. All these properties are due to the polarization dependence of geometric phase, which allows us to control the output image by changing the polarization of the input light.

4. RESULTS

4.1 Simulation Results

Based on the theory above, we retrieve the phase of the target image for the hologram using Gerchberg-Saxton algorithm and simulate the output image. We choose the target to be a half grid which can demonstrate both the wavelength dependence and polarization sensitivity at same time.

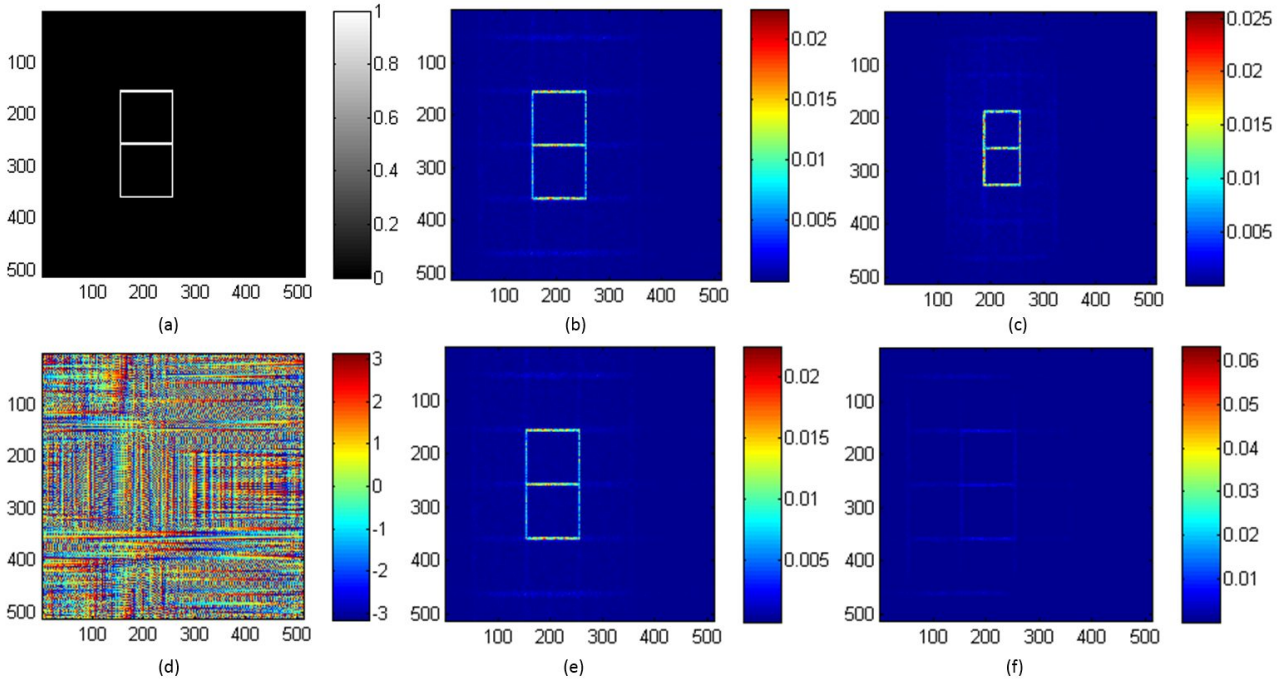

Figure 1. (a)Target image for $\lambda = 633nm$, (b)Replayed image of FGPH for $\lambda = 633nm$, (c)Replayed image of FGPH for $\lambda = 422nm$, (d)Phase profile of traditional FTH and FGPH for $\lambda = 633nm$, (e)Replayed image of traditional FTH for $\lambda = 633nm$, (f)Replayed image of traditional FTH for $\lambda = 422nm$. In (a) and (d), the color scale shows the target intensity and value of retrieved phase respectively. For (b), (c), (e) and (f), the color scale represents the relative magnitude of electric field.

In Figure 1 we firstly show the target image which is a half grid with 512×512 pixels. The retrieved phase profile of the target is also given and we know that it works for both traditional FTH and FGPH if the replay wavelength is $633nm$. Besides this, we can verify the wavelength dependence of the FGPH from the other four figures, which are calculated by taking the Fourier transform of the electric field at the hologram plane. From Figure 1 (b) and (e), we know the output far-field image will be identical for traditional FTH and FGPH at the desired replay wavelength, which matches our expectation.

When the replay wavelength is changed to a smaller value $422nm$ compared to the original value, for FGPH the phase profile keeps the same since the geometric phase is wavelength independent. Therefore, the new output image is a scaled version of the original image without chromatic distortion which matches the theoretical prediction well. This is shown clearly in Figure 1 (c). On the other hand, with the change of the replay wavelength, the phase profile of the traditional FTH has to change given the definition of the dynamic phase $\phi_d = 2\pi nd/\lambda$. With the change in phase at the hologram plane, the reconstructed image of the traditional Fourier Transform hologram suffers from chromatic distortion inevitably and becomes hard to distinguish it from the noise, which is verified in Figure 1 (f).

4.2 Experimental Results

We experimentally realized FGPH formed as liquid crystal thin films fabricated by a direct-writing system using photoalignment techniques. We utilized a linear photopolymerizable polymer(LPP):LIA-C001(DIC Corporation, Japan Ltd.) as the photoalignment material . The surface alignment pattern was recorded in the LPP layer using a UV laser (355 nm). After the UV exposure of LPP, liquid crystal polymer (LCP) was spin-coated onto the patterned LPP-coated substrate. We utilized RMS10-25 ($\Delta n = 0.16$ at 589 nm, Merck Chemicals, Ltd.) to create this birefringent LCP film. A mixture (1:3 of RMS10-25:) layer was first coated to improve later coating quality. Spin-coating speeds were 1500 rpm for the LPP layer and 900 rpm for the LCP layer, respectively.

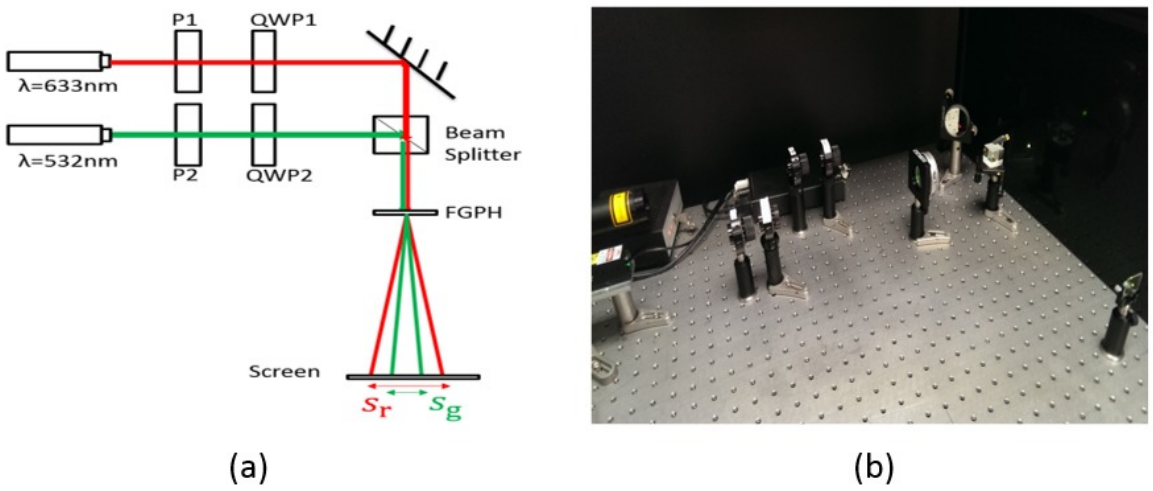

Figure 2. (a) and (b) are the illustration and photo of the characterization setup

To characterise the FGPH, we collimated the red and green laser beams and illuminated the sample with the two beams. Photos were taken for the far-field images using a camera and we also measure the size of the image given by each wavelength.The ratio of the sizes is $s_r/s_g = 0.82$ which is very close to the ratio of the two wavelengths $\lambda_r/\lambda_g = 0.84$. This result matches the theoretical prediction very well.

From the results in Figure 3, opposite circular polarized input will have opposite diffraction angle, which validates the polarization sensitivity. Since the linear polarized light is a superposition of LCP and RCP light, its output image is a combination of the two, which looks like a full grid. Since the traditional Fourier Transform hologram utilizes dynamic phase which is not polarization sensitive, its output image will not be changed by the input polarization.

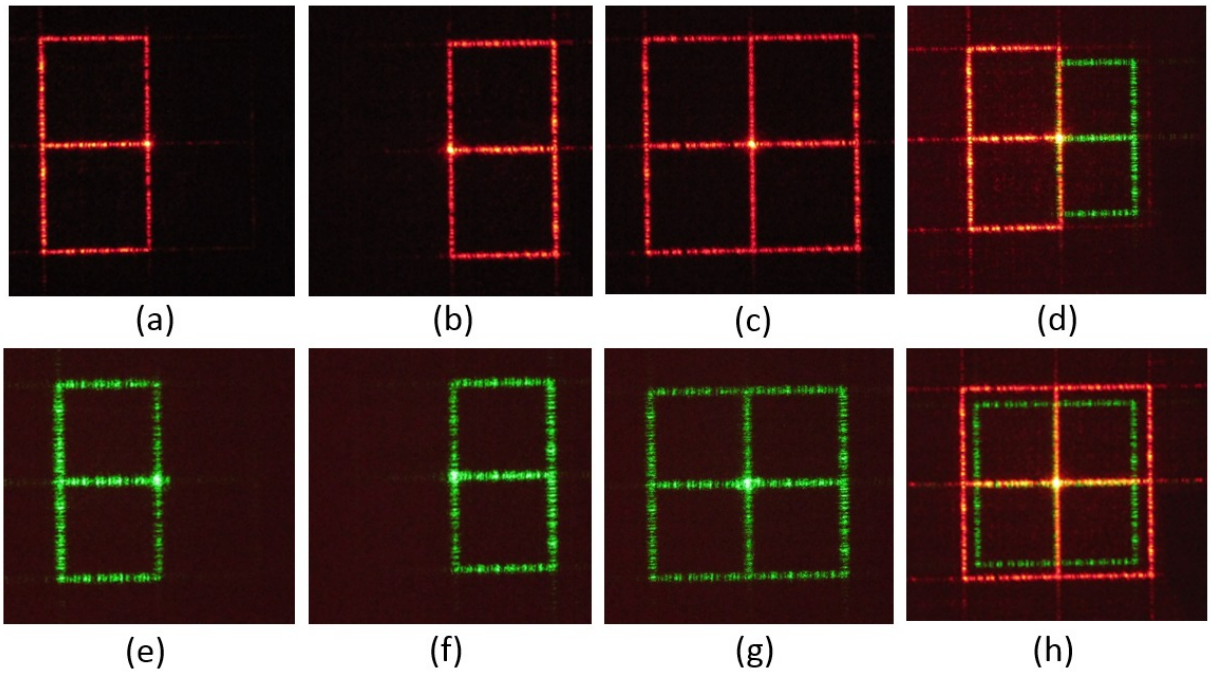

Figure 3. Replayed images for (a)Red RCP input, (b)Red LCP input, (c)Red LP input, (d)Red RCP and green LCP input, (e)Green RCP input, (f)Green LCP input, (g)Green LP input, (h)Red and Green LP input.

Besides the validation of the polarization dependence, we can also verify the wavelength dependence. For the traditional Fourier transform hologram, we have known that the output image will suffer from chromatic distortion and become hard to preserve the high contrast if the replay wavelength is different from the record wavelength. However, the reconstructed image of green laser is indeed a scaled version of the one given by the red laser and it is able to keep high contrast without chromatic distortion.

The zero order in the output image has no information of the hologram and can be minimized by optimized the thickness of the FGPH.

5. CONCLUSIONS

We proposed a new kind of 2D Fourier transform hologram using geometric phase and have successfully realized it. We demonstrated unique optical properties of the FGPH in theory and corresponding simulations were performed based on the theoretical results. We also fabricated FGPH samples using the direct-writing system and all predicted properties were validated. Besides the wavelength and polarization dependence, the FGPH also shows high diffraction efficiency which should be even better if the thickness is optimized to minimize the zero order.

APPENDIX A. GEOMETRIC PHASE VIA A RETARDER

We firstly consider the change in polarization to a plane wave traveling in z direction after passing through a retarder located at z = 0 with thickness d, birefringence Δn, and optical axis θ. The input wave is assumed to be right circular polarized neglecting the phase constant. We also assume that a reference wave is also RCP, but passes through an identical medium except the medium has optical axis $\theta_r = 0$. After applying the Jones calculus method, the output Jones vector after passing through the retarder is:

$$\mathbf{J_{out}} = \frac{1}{\sqrt{2}} \begin{pmatrix} 1 \\ i \end{pmatrix} \begin{pmatrix} e^{i\phi_e}\cos^2\theta + e^{i\phi_o}\sin^2\theta & (e^{i\phi_e} - e^{i\phi_e})\cos\theta\sin\theta \\ (e^{i\phi_e} - e^{i\phi_e})\cos\theta\sin\theta & e^{i\phi_e}\sin^2\theta + e^{i\phi_o}\cos^2\theta \end{pmatrix} \tag{10}$$

where $\phi_e = 2\pi(n_o + \Delta n)d/\lambda$ and $\phi_o = 2\pi n_o d/\lambda$. Notice that $\phi_e = \phi_o + 2\pi\zeta$, where $\zeta = \Delta n d/\lambda$ is the retardation. After simplification of the matrix, we obtain:

$$\mathbf{J_{out}} = \frac{e^{i\phi_o}}{\sqrt{2}} \begin{pmatrix} e^{i2\pi\zeta}(\cos^2\theta + i\sin\theta\cos\theta) + (\sin^2\theta - i\sin\theta\cos\theta) \\ e^{i2\pi\zeta}(\sin\theta\cos\theta + i\sin^2\theta) + (-\sin\theta\cos\theta + i\cos^2\theta) \end{pmatrix} \tag{11}$$

Given the Jones vectors of RCP and LCP, we can rewrite the result above in the form of superposition of these two orthogonal bases:

$$\mathbf{J_{out}} = \frac{e^{i\phi_0}}{2\sqrt{2}}[(e^{i2\pi\zeta} + 1)\begin{pmatrix} 1 \\ i \end{pmatrix} + (e^{i2\pi\zeta} - 1)e^{i2\theta(x',y')}\begin{pmatrix} 1 \\ -i \end{pmatrix}] \tag{12}$$

ACKNOWLEDGMENTS

Matthew N. Miskiewicz and Michael J. Escuti gratefully acknowledge the support of the National Science Foundation (CAREER award ECCS-0955127), and Xiao Xiang and Michael J. Escuti acknowledge the financial support of ImagineOptix Corporation, within which M.J.E. holds an equity interest. The authors also acknowledge Dr Jihwan Kim for helpful discussions.

REFERENCES

[1] Anandan, J., "The geometric phase," *Nature* **360**, 307313 (1992).
[2] Bhandari, R., "Polarization of light and topological phases," *Physics Reports* **281**, 1–64 (1997).
[3] Berry, M., "Anticipations of the geometric phase," *Physics Today* **43**, 34 (1990).
[4] Miskiewicz, M. and Escuti, M. J., "Direct-writing of complex liquid crystal patterns," *Optics Express* **39**, 1521–1524 (2014).
[5] Lee, W. H., "Sampled fourier transform hologram generated by computer," *Applied Optics* **9**, 639–643 (1970).
[6] Lohmann, A. W. and Paris, D. P., "Binary fraunhofer holograms, generated by computer," *Applied Optics* **6**, 1739–1748 (1967).
[7] F. Wyrowski, R. H. and Bryngdahl, O., "Computer-generated holography: hologram repetition and phase manipulations," *J. Opt. Soc. Am. A* **4**, 694698 (1987).
[8] Fahri Yara, H. K. and Onural, L., "Real-time phase-only color holographic video display system using led illumination," *Applied Optics* **48**, 34 (2005).
[9] Gerchberg, R. W. and Saxton, W. O., "A practical algorithm for the determination of the phase from image and diffraction plane pictures," *Optik* **35**, 237 (1972).
[10] Fienup, J. R., "Phase retrieval algorithms: a comparison," *Applied Optics* **21**, 2758–2769 (1982).
[11] Pedro Andr6s, J. L. and Furlan, W. D., "White-light fourier transformer with low chromatic aberration," *Applied Optics* **31**, 23 (1992).
[12] Padgett, M. J. and Courtial, J., "Poincaré-sphere equivalent for light beams containing orbital angular momentum," *OPTICS LETTERS* **24**, 430–432 (1999).
[13] Escuti, M. J. and Jones, W. M., "Polarization-independent switching with high contrast from a liquid crystal polarization grating," *SID Symposium Digest* **37**, 14431446 (2006).
[14] Yanming Li, J. K. and Escuti, M. J., "Orbital angular momentum generation and mode transformation with high efficiency using forked polarization gratings," *Applied Optics* **51**, 8236–8245 (2012).
[15] Erez Hasman, Zeev Bomzon, A. N. G. B. V. K., "Polarization beam-splitters and optical switches based on space-variant computer-generated subwavelength quasi-periodic structures," *Optics Communications* **209**, 4554 (2002).
[16] Todorov, T., N. L. S. K. . T. N., "Polarization holography. 3: Some applications of polarization holographic recording," *Applied Optics* **24**, 785788 (1985).
[17] Bryngdahl, O., "Polarization-grating moire.," *J. Opt. Soc. Amer.* **62**, 839848 (1972).